Check for updates

The proteomic characteristics of airway mucus from critical ill COVID-19 patients

Zili Zhang [1], Tao Wang [1], Fei Liu [1], Airu Zhu [1], Guoping Gu [1], Jieping Luo, Jingyi Xu, Jincun Zhao, Yiming Li, Yuanyuan Li, Xiaoqing Liu [*], Nanshan Zhong [*], Wenju Lu [*]

State Key Laboratory of Respiratory Diseases, Guangdong Key Laboratory of Vascular Diseases, National Clinical Research Center for Respiratory Diseases, Guangzhou Institute of Respiratory Health, the First Affiliated Hospital of Guangzhou Medical University, Guangzhou, Guangdong, China

ARTICLE INFO

ABSTRACT

Background: The pandemic of the coronavirus disease 2019 (COVID-19) has brought a global public health crisis. However, the pathogenesis underlying COVID-19 are barely understood.
Methods: In this study, we performed proteomic analyses of airway mucus obtained by bronchoscopy from severe COVID-19 patients. In total, 2351 and 2073 proteins were identified and quantified in COVID-19 patients and healthy controls, respectively.
Results: Among them, 92 differentiated expressed proteins (DEPs) (46 up-regulated and 46 down-regulated) were found with a fold change >1.5 or <0.67 and a *p*-value <0.05, and 375 proteins were uniquely present in airway mucus from COVID-19 patients. Pathway and network enrichment analyses revealed that the 92 DEPs were mostly associated with metabolic, complement and coagulation cascades, lysosome, and cholesterol metabolism pathways, and the 375 COVID-19 only proteins were mainly enriched in amino acid degradation (Valine, Leucine and Isoleucine degradation), amino acid metabolism (beta-Alanine, Tryptophan, Cysteine and Methionine metabolism), oxidative phosphorylation, phagosome, and cholesterol metabolism pathways.
Conclusions: This study aims to provide fundamental data for elucidating proteomic changes of COVID-19, which may implicate further investigation of molecular targets directing at specific therapy.

1. Introduction

Coronavirus disease 2019 (COVID-19) is an unprecedented global threat caused by severe acute respiratory syndrome coronavirus 2 (SARS-CoV-2). Currently, it is rapidly spreading around the world. As of December 30, 2020, there are over 82,051,958 confirmed COVID-19 cases and about 1,792,251 deaths worldwide according to the situation report by WHO. Based on a recent study of 44,672 confirmed COVID-19 cases up to February 11 by the Chinese Center for Disease Control and Prevention, over 19% of COVID-19 patients developed severe or critical conditions [1]. Moreover, the mortality rate of COVID-19 in critically ill cases can be over 60%, posing a great pressure on treatment [2]. However, the biochemical and molecular changes associated with the severe form of COVID-19 are barely understood.

In our clinic, we found it is common that the small airway and alveolar wall of critical ill COVID-19 patients were blocked with thick and sticky mucus, which contributes to the causes of difficult breathing [3]. In this study, we speculated that these mucus are a mixture of secretion by airway and alveolar epithelial cells in response to virus and inflammatory mediators, and the molecular changes may indicate the pathological changes of COVID-19. Proteomics is the huge fields that are equipped with sufficient technologies to face this challenge. Therefore, proteomics analysis was performed with the aim to provide fundamental information for understanding the pathogenesis of COVID-19, and for future development of therapeutic approaches.

2. Material and methods

2.1. Study design and clinical data collection

In our critical care units, the critical ill COVID-19 patients suffered from expectoration difficulty and dyspnea were treated with

bronchoscopy to aspirate the airway mucus. The bronchoscopy operation was carried out using a PENTAX FB-15BS portable fiber bronchoscopy (PENTAX Medical Shanghai Co, Ltd., Shanghai, China) through tracheal intubation. Subjects negative for the SARS-CoV-2 nucleic acid test and absent of lung disease condition were included as controls. For the healthy control subjects, airway mucus was induced by hypertonic (3%) saline solution inhalation delivered with an ultrasonic nebulizer.

We reviewed clinical charts, nursing records, laboratory findings, and chest imaging of all patients with laboratory-confirmed SARS-CoV-2 infection who were reported by the local health authority. The admission data of these patients were from January 26, 2020, to February 15, 2020. Data regarding epidemiological, clinical, laboratory and radiological characteristics were obtained from electronic medical records. Two researchers independently reviewed the data collection forms to double-check the collected data. All the procedures were approved by the Ethics Committee of the First Affiliated Hospital of Guangzhou Medical University (No. 2020-65). Verbal informed consent were obtained from all participants because the family members were in quarantine.

2.2. Airway mucus processing

The airway mucus was processed according to a previously published procedure [4]. Briefly, the airway mucus was weighed, added with equal volume of PBS, and incubated for 15 min at 4 °C with vigorous shaking. Afterwards, the suspension was filtered through a 74-μm Nylon mesh (Chemical Instrument Company, Beijing, China), and the filtrate was centrifuged at 790g for 10 min. The resultant supernatant was then aliquoted, denatured at 56 °C for 45 min, and stored at −80 °C for subsequent proteomic analysis.

2.3. Protein extraction and trypsin digestion

Airway mucus processed with above procedure was sonicated three times on ice using a high intensity ultrasonic processor (Scientz) in lysis buffer (8 M urea, 1% Protease Inhibitor Cocktail). The remaining debris was removed by centrifugation at 12,000g at 4 °C for 10 min. Finally, the supernatant was collected and the protein concentration was determined with BCA kit according to the manufacturer's instructions. For digestion, the protein solution was reduced with 5 mM dithiothreitol for 30 min at 56 °C and alkylated with 11 mM iodoacetamide for 15 min at room temperature in darkness. The protein sample was then diluted by adding 100 mM TEAB to urea concentration less than 2 M. Finally, trypsin was added at 1:50 trypsin-to-protein mass ratio for the first digestion overnight and 1:100 trypsin-to-protein mass ratio for a second 4 h-digestion.

2.4. Quantification of proteomic data and LC-MS/MS analysis

For label-free quantification, protein expression levels were estimated using the iBAQ (Intensity Based Absolute Quantification) algorithm embedded in MaxQuant [5]. Briefly, normalization and the intensity-based absolute quantification (iBAQ) in MaxQuant was performed on the identified peptides to quantify protein abundance. In particular, shared peptides, which matched different protein groups, were excluded from quantification. Only proteins with a fold change >1.5 or <0.67 and a p-value <0.05 in at least two biological replicates were considered to exhibit a significant difference in protein abundance between the two groups.

The peptides were subjected to NSI source followed by tandem mass spectrometry (MS/MS) in Q ExactiveTM Plus (Thermo) coupled online to the UPLC. Peptides were then selected for MS/MS using NCE setting as 28 and the fragments were detected in the Orbitrap at a resolution of 17,500. Principal Components Analysis (PCA) was performed to visualize separation of COVID-19 patients and controls.

2.5. Pathway analysis

Gene Ontology (GO) annotation proteome was derived from the UniProt-GOA database (http://www.ebi.ac.uk/GOA/). Proteins were classified by GO annotation into three categories: biological process, cellular compartment, and molecular function. For each category, a two-tailed Fisher's exact test was employed to test the enrichment of the differentially expressed protein (DEPs) against all identified proteins. The GO with a corrected p-value of <0.05 was considered significant. Kyoto Encyclopedia of Genes and Genomes (KEGG) database was used to identify enriched pathways. In this context, we used the two-tailed Fisher's exact test to examine the enrichment of the DEPs against all identified proteins. The pathway with a corrected p-value of <0.05 was considered significant. All DEPs database accession or sequence were searched against the STRING database version 10.1 for protein-protein interactions (PPI). Meanwhile, STRING defines a metric called "confidence score" to define interaction confidence; we fetched all interactions that had a confidence score of ≥0.7 (high confidence). Interaction network form STRING was visualized in R package "networkD3". For further hierarchical clustering based on DEPs functional classification. Cluster membership were visualized by a heat map using the "heatmap.2" function from the "gplots" R-package.

2.6. Statistical analysis

Continuous variables were presented as median (IQR). Categorical variables were presented as n (%). All analyses were done with Graph-Pad Prism 5 software, using two-sided p values. Statistical significance was set at $p < 0.05$.

3. Results

3.1. Clinical characteristics of COVID-19 subjects

The clinical characteristics of COVID-19 patients and healthy controls are shown in Table 1. There were no significant differences regarding baseline characteristics between both groups as regards to age, gender, and smoking status. All COVID-19 patients were admitted to the intensive care unit (ICU) because of acute respiratory distress syndrome (ARDS) comorbidity (100%) and diabetes (20%), and all of them had polypnea with lymphocytopenia (0.3 × 10 [9]/L with IQR 0.25–0.55, $n = 5$) and extremely elevated lactate dehydrogenase (397 U/L with IQR 356–535, $n = 5$) and D-dimer (1390 μg/mL with IQR 741–4667, n = 5) levels. Blood laboratory tests showed elevated inflammatory indexes, including white cell count (11.1 × 10 [9]/L with IQR 7.30–12.8, $n = 5$) and interleukin-6 (IL-6) (22.2 pg/mL with IQR 9.40–60.0, n = 5) in COVID-19 patients. In addition, the chest CT scans of all patients revealed the characteristic imaging features of COVID-19 in the forms of consolidation, ground-glass opacity, and bilateral pulmonary infiltration.

3.2. Proteomic profiling of airway mucus from COVID-19 patients

Airway mucus samples were obtained from five critical ill COVID-19 patients and 5 healthy controls. Label-free quantification of proteomic were used to analyze airway mucus from each individual. The airway mucus from COVID-19 patients displayed distinct proteomic patterns compared to controls. In total, 2351 and 2073 proteins were identified and quantified in the airway mucus from COVID-19 patients and healthy controls, respectively. The proteomics datasets (including fold-change and p-values for the two groups comparisons) are provided in Table S1. In the quality control analysis, PCA, the median Relative SD (RSD) of all internal standards in each sample, protein mass and coverage distribution, and protein sequence distribution were calculated (Fig. S1). Our data were acquired with a high degree of consistency and reproducibility.

Table 1
Demographic, clinical, laboratory and radiographic findings of patients.

	Total	COVID-19	Health	p value
	$n = 10$	n = 5	n = 5	
Demographics and clinical characteristics				
Age, years		70(66–72)	69 (63–75)	0.94
Male	7(70.0)	5(100.0)	2(40.0)	0.71
Death	0	0	0	–
ICU admission	5(50.0)	5(100.0)	0	–
ICU length of stay, days	37 (10–43)	37(10–43)	–	–
Hospital length of stay, days	45 (41–48)	45(41–48)	–	–
Time from illness onset to hospital admission, days	57 (53–68)	57(53–68)	–	–
Severe	5(50.0)	5(100.0)	0	–
Ever smoke	6(60.0)	4(80.0)	2(40.0)	0.87
Comorbidity				
Diabetes	1(20.0)	1(20%)	0	
ARDS	5(100.0)	5(100%)	0	
Respiratory rate	20 (14–20)	20(14–20)	–	–
>24 breaths per min	1(10.0)	1(20.0)	0	–
Pulse ≥100 beats per min	1(10.0)	1(20.0)	0	–
O_2 pressure	–	82.8 (69.0–110.0)	–	–
O_2 concentration	–	95.3 (93.3–95.4)	–	–
Fever (temperature ≥ 37.3 °C)	1(10.0)	1(20%)	0	–
Cough	4(80.0)	4(80.0)	0	–
Sputum	0	0	0	–
Myalgia	0	0	0	–
Fatigue	2(40.0)	2(40.0)	0	–
Diarrhoea	0	0	0	–
Vomiting	0	0	0	–
Rhinobyon	0	0	0	–
Hemoptysis	0	0	0	–
Headache	0	0	0	–
Sorethroat	1(10.0)	1(20.0)	0	–
Polypnea	5(100.0)	5(100.0)	0	–
Shiver	0	0	0	–
Laboratory findings				
White blood cell count, ×10⁹/L	–	11.1 (7.30–12.8)	–	–
Lymphocyte count, ×10⁹/L	–	0.30 (0.25–0.55)	–	–
Monocyte count, ×10⁹/L	–	0.40 (0.35–0.65)	–	–
Platelet count, ×10⁹/L	–	117.0 (87.0–212.5)	–	p
Lactate dehydrogenase, U/L	–	397(356–535)	–	–
High-sensitivity cardiac	–	0.01 (0.005–0.03)	–	–
Troponin I, pg/mL	–		–	–
Prothrombin time, s	–	15.7 (13.6–18.1)	–	–
D-dimer, μg/mL	–	1.39 (0.74–4.67)	–	–
IL-6, pg/mL	–	22.2 (9.40–60.0)	–	–
Procalcitonin, ng/mL	–	0.27 (0.09–0.43)	–	–
CRP	–	2.7(1.5–12.9)	–	–
DBIL	–	4.1(3.0–8.7)	–	–
TBIL	–	13.6 (11.9–20.4)	–	–
CK-MB	–	11.0(7.0–18.0)	–	–
Cr	–	77.0 (69.1–91.7)	–	–
Imaging features				
Consolidation	5(50.0)	5(100.0)	0	–
Ground-glass opacity	5(50.0)	5(100.0)	0	–
Bilateral pulmonary infiltration	5(50.0)	5(100.0)	0	–

Data are median (IQR) or n (%). P values were calculated by Mann-Whitney *U* test or Fisher's exact test, as appropriate.

3.3. Identification and enrichment analyses of COVID-19 unique proteins

In the proteomic datasets, there was a total of 375 proteins uniquely present in the mucus from COVID-19 patients but not in controls (Table S2, Fig. 1A). Out of them, 28.19% were located in the cytoplasm, 20.48% in extracellular, and 16.22% in the nucleus (Fig. 1B, E). As illustrated in Fig. 1D and G, the biological process analysis revealed that these proteins were enriched in granulocyte activation, neutrophil mediated immunity, myeloid leukocyte activation, and carboxylic acid metabolic processes. The molecular function analysis indicated that they were mainly distributed in three function processes: hydrogen ion transmembrane transporter activity, electron carrier activity, and antigen binding. KEGG pathway analyses demonstrated that there were five pathways enriched: amino acid degradation (valine, leucine and isoleucine degradation), amino acid metabolism (beta-Alanine, tryptophan, cysteine and methionine metabolism), oxidative phosphorylation, phagosome, and cholesterol metabolism (Fig. 1C). From these pathway analyses, the proteins with high frequency existence in at least two pathways were ACADS, ACAT1, ACTG1, ALDH2, ALDH3A2, ALDH6A1, ATP5F1C, CASP8, COX5B, COX6B1, CYC1, DLD, HADH, HADHA, HLA-DMB, HLA-DRB1, MT-CO3, NDUFS1, SLC25A5, SLC25A6, UQCRC2, VDAC1 and VDAC1-3 (Fig. 1H).

3.4. Identification and enrichment analyses of these differential expressed proteins

In the above proteomic datasets, 92 differential expressed proteins (DEPs) between two groups were identified (Fig. 2A-D), including 46 up-regulated and 46 down-regulated proteins in the mucus from COVID-19 group with a fold change ≥1.5 or ≤0.67 and a *p*-value <0.05 (Fig. 2A-D). A total of 43.48% of these proteins were distributed in extracellular compartment, 25% in cytoplasm, and 13.04% in nucleus (Fig. 2E). Out of the 92 DEPs, 33 of them (35%) were present in at least two pathways (Fig. 3A). Pathway and network enrichment analyses revealed that most of these DEPs were associated with metabolic, complement and coagulation cascades, lysosome, and cholesterol metabolism pathways (Fig. 3B). Among them, the top ten ranked proteins were LAMP2, TYMP, CTSS, PLTP, HBA1, and RAB11B according to differential significance level (Fig. 3C) and ASS1, FGG, GOT1 and ALDH3A1 by high-frequency existence in at least two pathways (Fig. 3D).

Next, GO and KEGG functional enrichment analyses were performed to annotate the potential functional implication of these differently grouped DEPs, which revealed that protein activation cascade, immunoglobulin mediated immune response, B cell mediated immunity, and leukocyte migration processes were enriched; most of these proteins were also located in extracellular space, cytoplasm, and extracellular. The molecular function of these proteins was primarily distributed on three function processes: serine-type peptidase activity, serine-type endopeptidase activity, and serine hydrolase activity (Fig. 4A-C). KEGG pathway and heatmap analyses revealed that these DEPs were significantly enriched in amino acid metabolism (phenylalanine/arginine biosynthesis/tyrosine) and cholesterol metabolism (Figs. 4D and 5). Therefore, the final dysregulated proteins were selected, including GOT1, ALDH3A1, ASS1, APOH, PLTP1, and APOB from KEGG (Fig. 4E, F); SERPINA1, FGG, FGB, ORM1, and AHSG based on PPI networks, which had maximum number of nodes (Fig. 4H, G).

GO enrichment analysis was also conducted for the 46 up-regulated proteins and the 46 down-regulated proteins, respectively (Fig. 6A, C). For the 46 up-regulated proteins, the significantly altered molecular function terms comprised: (a) serine-type endopeptidase activity, (b) serine-type peptidase activity, serine hydrolase activity, and (c) antigen binding; the biological process terms comprised: (a) blood coagulation, fibrin clot formation, (b) regulation of blood vessel size, (c)
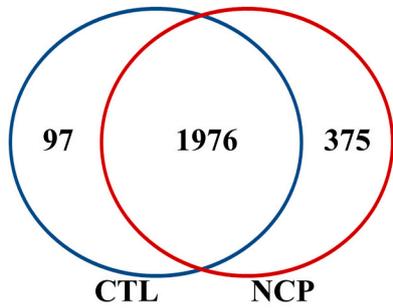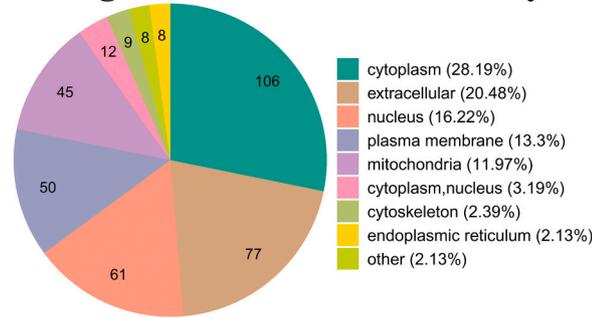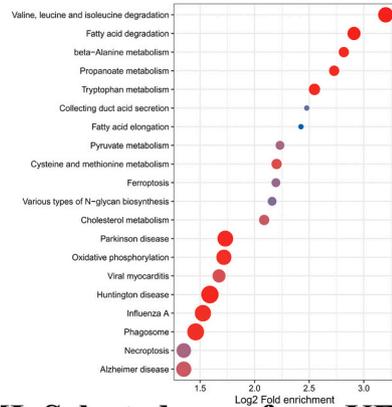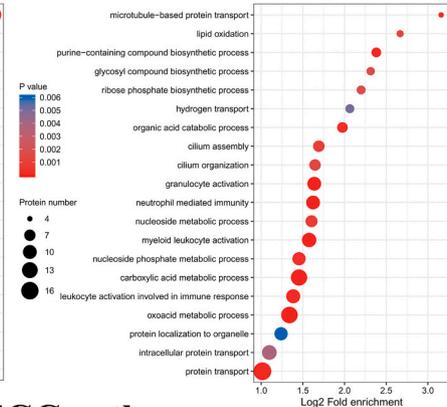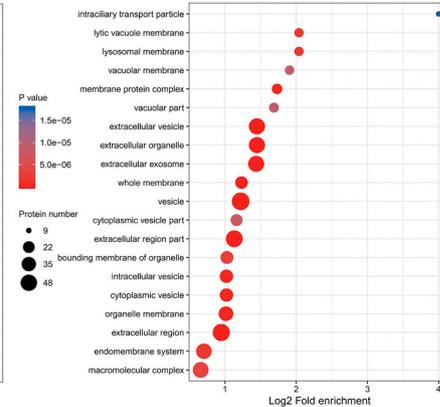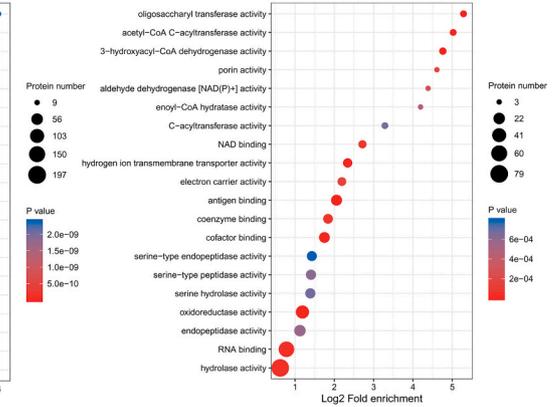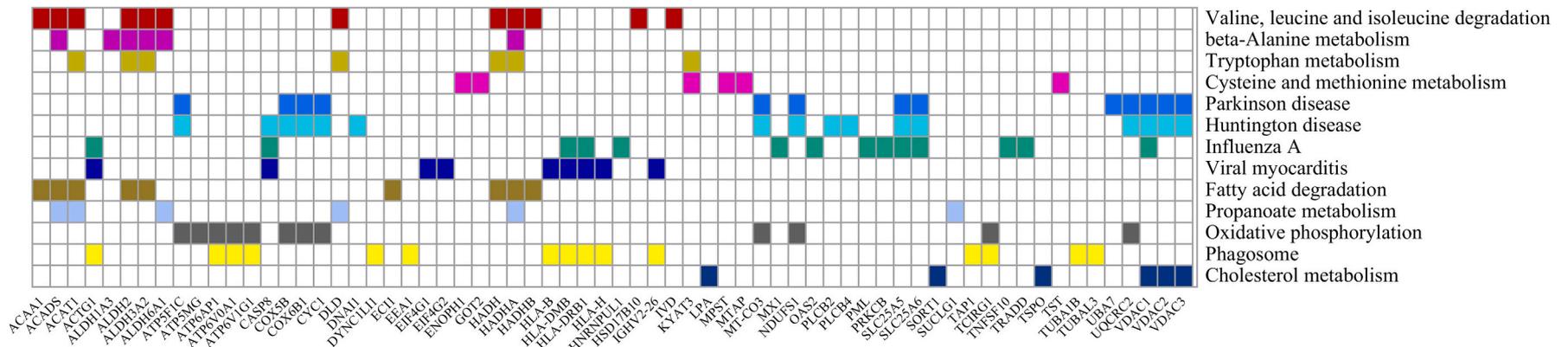
Fig. 1. Proteins analysis showed unique to COVID-19 patients (NCP) (375 proteins): A. Venn plot, identification of the NCP-specific proteins between NCP and controls by overlapping them; B. subcell classify of these unique genes for NCP; C. the proteome KEGG enrichment analysis of NCP; D, E and G: Gene Ontology (GO) annotation for biological process, cellular compartment, and molecular function, respectively.
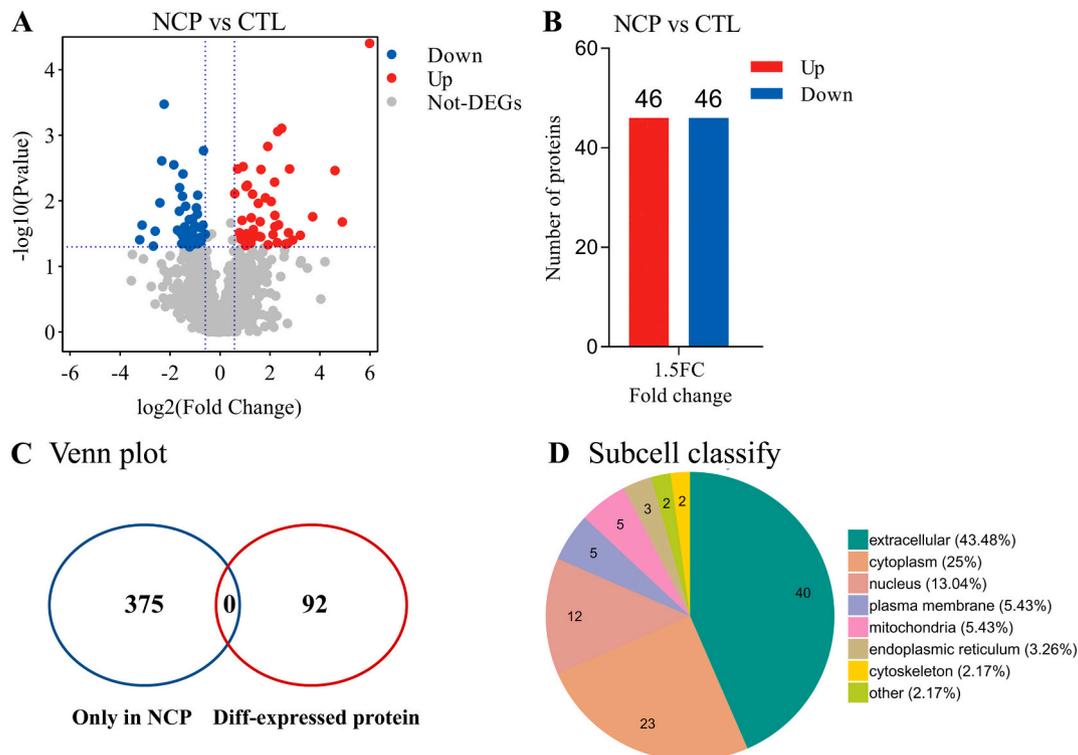
Fig. 2. Differentiated expressed proteins (DEPs) analysis between COVID-19 patients (NCP) and control group (CTL) (92 proteins). A. The volcano plot; blue: down-regulation proteins; red: up-regulation proteins; B. protein number for each up- and down-regulation protein group, respectively (with a fold chang >1.5 or < 0.67 and a *p*-value <0.05); C. Venn plot, identification of the common proteins between NCP and controls by overlapping them; D. subcell classify of these DEPs. (For interpretation of the references to colour in this figure legend, the reader is referred to the web version of this article.)

Antimicrobial humoral response, (d) protein activation cascade, (e) immunoglobulin mediated immune response, (f) B cell mediated immunity, and (g) receptor-mediated endocytosis. Most of them were located in extracellular space. For the 46 down-regulated proteins, the molecular function terms mainly involved: growth factor activity. The biological process terms involved: (a) maintenance of apical/basal cell polarity, (b) retrograde tansport, endosome to plasma membrane, (c) plasma membrane tubulation, and (d) fructose 1,6-bisphosphate metabolic process. As shown in Fig. 6B, D, the network was enriched for the following pathways (for the up-regulated proteins): (a) arginine biosynthesis, (b) alanine, aspartate and glutamate metabolism, (c) cholesterol metabolism, and (d) complement and coagulation cascades. Pathway enrichment for the 46 down-regulated proteins were primarily distributed on glycolysis/gluconeogenesis.

4. Discussion

We report here a proteomic analysis of airway mucus obtained by bronchoscopy from 5 COVID-19 patients with laboratory-confirmed SARS-CoV-2 infection. The results revealed that these dysregulated proteins were mainly enriched in two functional pathways: metabolic pathways, and complement and coagulation cascade pathways.

For COVID-19 patients, the metabolisms such as amino acids, nucleotides, organic acids, and carbohydrates were greatly reduced. Simultaneously, the lipids involved in the cholesterol metabolism pathway were upregulated, which maintains the balance of the energy metabolites of the body and are beneficial to the energy required for viral replication, implying that SARS-CoV-2 probably hijacks cellular metabolism like many other viruses [6]. Our data also found a generalized reduction in metabolic proteins, including FBP1, ALDOC, NAGA, TYMP, ALDH3A1, CHMP4B and NAGK, and an upregulation of cholesterol proteins as APOB and PLTP. For instance, FBP1(Fructose-Bisphosphatase 1), a gluconeogenesis regulatory rate-limiting enzyme,

can catalyze the hydrolysis of fructose 1,6-bisphosphate to fructose 6-phosphate and inorganic phosphate [7,8]. Among its related pathways are Glucose metabolism and Carbon metabolism. FBP1 deficiency is associated with hypoglycemia and metabolic acidosis [9]. ALDOC (Aldolase, Fructose-Bisphosphate C) is a glycolytic enzyme that catalyzes the reversible aldol cleavage of fructose-1,6-biphosphate and fructose 1-phosphate to dihydroxyacetone phosphate and either glyceraldehyde-3-phosphate or glyceraldehyde, respectively [10]. This protein is related with innate immune system and Glucose metabolism pathways [11,12]. GO annotations related to ALDOC include cytoskeletal protein binding and fructose-bisphosphate aldolase activity. The findings suggest that the conditions caused by COVID-19 might be related with hepatic functions impairment. These dysregulated reduced proteins would provide hints of the pathogenesis of COVID-19, and be used for future development of therapeutic approaches.

Evidence revealed that the complement system plays pivotal roles in linking innate and adaptive immunity and that inflammation could aggravate the lung injury [13,14]. In particular, the role of immunity, such as complement activation, is considered cumulatively in conditions including ARDS, pneumonia, asthma, pulmonary arterial hypertension (PAH), and chronic obstructive pulmonary disease (COPD) [15]. In this study, an increased complement system proteins C9 were identified. Suppression of the complement system has been demonstrated as an effective immunotherapeutic in the SARS-infected mouse model [16]. In addition, FGB and FGG are important for blood clot formation (coagulation), and we found a general up-regulation of these proteins. Previous proteomic analysis (label-free) of plasma exosomes showed that the expression of FGG and FGB was significantly higher in the malignant pulmonary nodules group, compared to the benign pulmonary nodules group [17]. In lung cancer, FGB and FGG were one of the key epithelial-mesenchymal transition effectors associated with cell adhesion and cellular communication. We suggest that severe COVID-19 patients might benefit from the suppression of the complement and coagulation
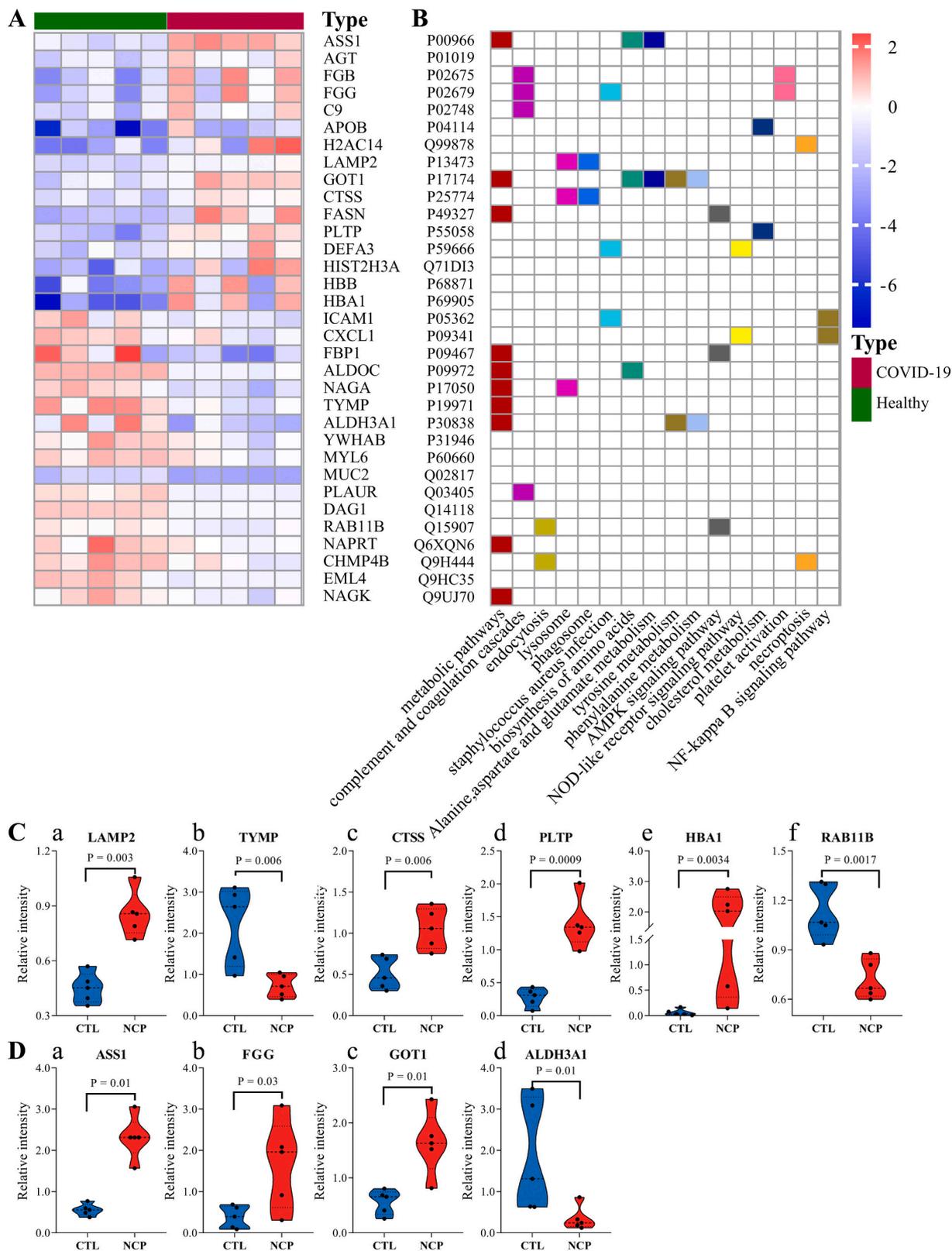
Fig. 3. Differentiated expressed proteins (DEPs) analysis between COVID-19 patients (NCP) and control group (CTL). A. Hierarchical clustering analysis of DEPs. Heatmap of the top 33 DEPs. The red colour in the heatmap denotes higher gene expression, and the blue colour in the heatmap denotes the lower gene expression. Target proteins symbols for the top 33 DEPs are involved; B. these dysregulated proteins concentrated mainly on two enriched pathways: metabolic pathways, and complement and coagulation cascades pathways (with DEPs high-frequency existence in the two pathways); C. the expression level change (original value) of ten selected proteins with significance indicated by the *p*-value. (For interpretation of the references to colour in this figure legend, the reader is referred to the web version of this article.)
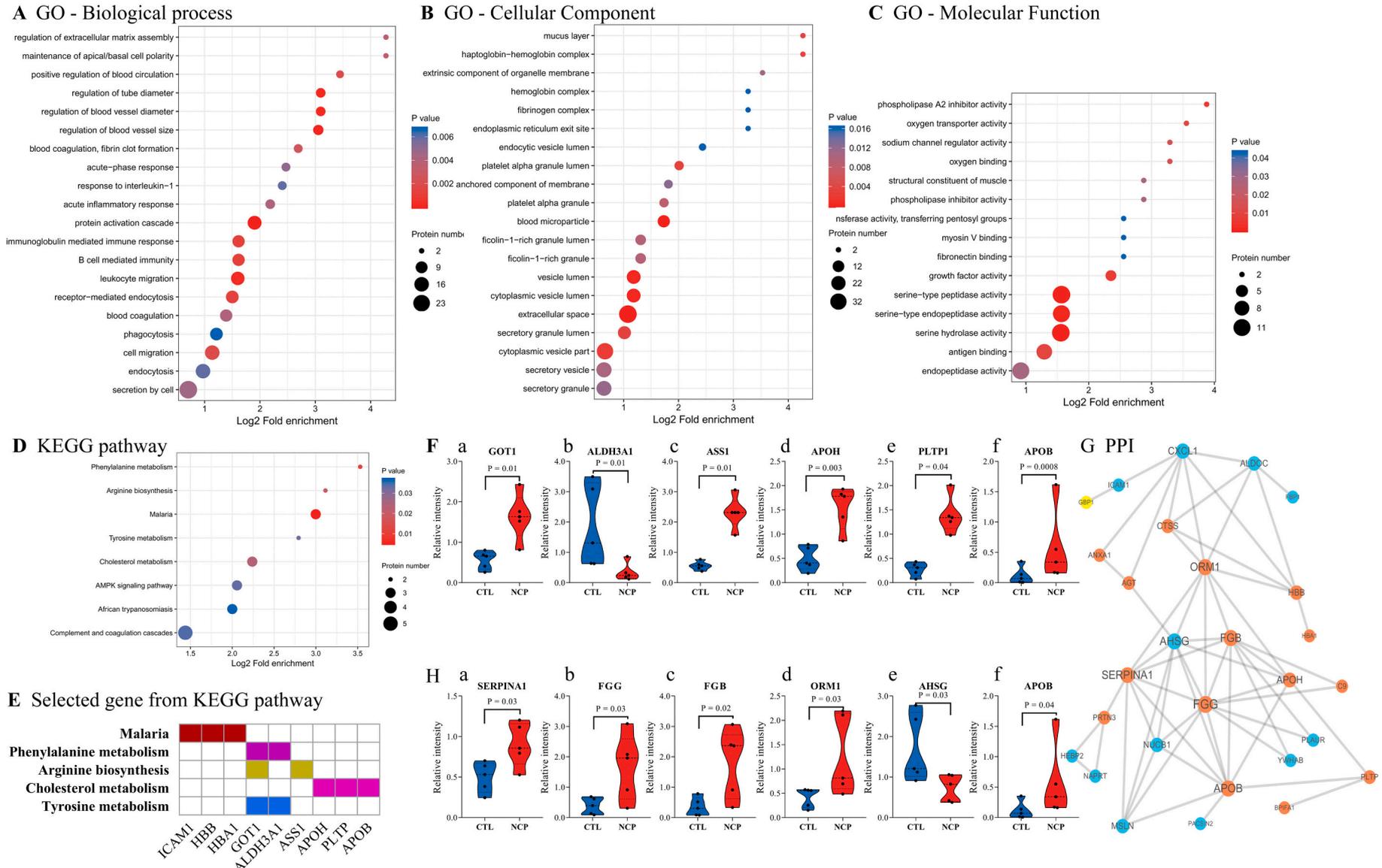
Fig. 4. GO and KEGG enrichment scatter plot of the Differentiated expressed proteins (DEPs). The y-axis shows significantly enriched GO and pathway terms relative to the network, and the x-axis shows the enrichment scores of these terms. Dot size represents the number of genes, and the colour indicates the *p*-value. A, B and C represent Gene Ontology (GO) annotation for biological process, cellular compartment, and molecular function, respectively; D. KEGG pathway analysis of DEPs; E. proteins selected from KEGG pathway; F. the expression level change (original value) of ten selected proteins with significance indicated by the p-value based on KEGG pathway; H. the expression level change (original value) of ten selected proteins with significance indicated by the p-value based on Protein-protein interaction (PPI) network; G. PPI of these DEPs constructed by STRING. Interactions at high confidence (score > 0.7) were considered. Nodes with no or scattered interactions were excluded.
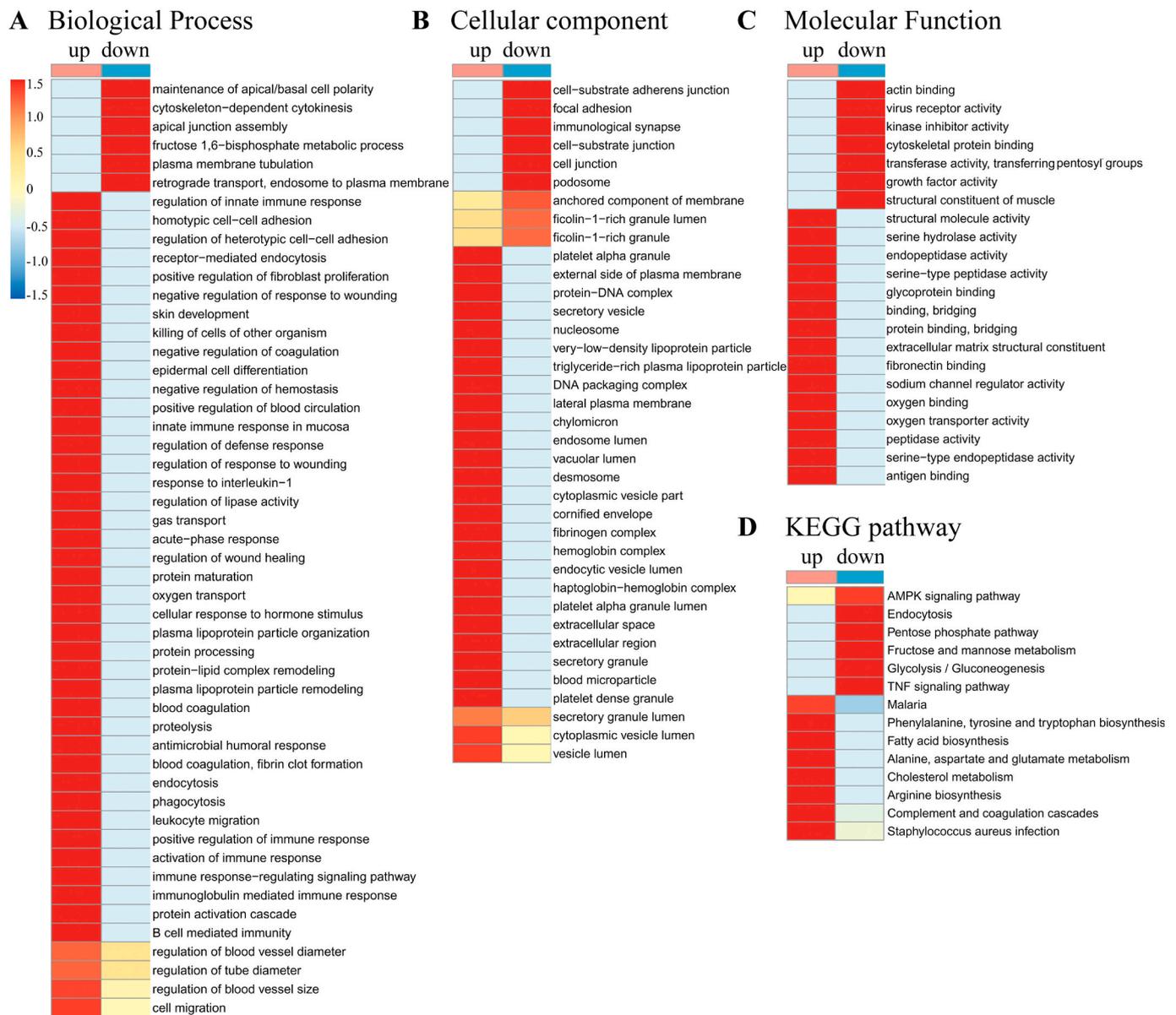
Fig. 5. Heatmap of differentiated up- and down-expressed proteins analysis on GO and KEGG. A, B and C represent Gene Ontology (GO) annotation for biological process, cellular compartment, and molecular function, respectively; B: KEGG pathway analysis of these differentiated up- and down-expressed proteins. Pink: up-regulated proteins; blue: down-regulated proteins. (For interpretation of the references to colour in this figure legend, the reader is referred to the web version of this article.)

systems.

In addition, amino acid metabolism (including phenylalanine metabolism, arginine biosynthesis, tyrosine metabolism), lysosome, and phagosome pathways were also significantly enriched. These dysregulated proteins included GOT1, ALDH3A1, ASS1, APOH, PLTP, APOB, NAGA, CTSS, LAMP2, ICAM1, DEFA3 and FGG.

Moreover, this retrospective study identified several risk factors for COVID-19 patients. In particular, D-dimer levels greater than 1 μg/mL, elevated levels of white blood cell counts, blood IL-6 and lactate dehydrogenase, and lymphocytopenia were more commonly seen in severe COVID-19 illness. We found that these above risk factors were associated with the outcomes of COVID-19 and were consistent with studies published [18–24].

Our study has some limitations. First, for all patients, airway mucus obtained by bronchoscopy, which might be a mixture of secretion by airway and alveolar epithelial cells in response to virus and inflammatory mediators. But for healthy controls, it was not ethical to obtain airway mucus via bronchoscopy, therefore induced sputum was used instead, and the content and counts of sputum cell may be different. Second, because this study is retrospective, not all laboratory tests were done in all participants such as IL-6, D-dimer and lactate dehydrogenase. Therefore, their influences on outcomes might be underestimated. Third, with the limited number of participants, it is difficult to assess host risk factors for disease severity with multivariable adjusted methods. Collection of standardized data from a larger cohort with a full picture of the spectrum of clinical severity combined with proteomic data would help to better understand the pathogenesis of this disease.

5. Conclusion

The proteomic datasets of COVID-19 patients' airway mucus are highly valuable resources for better understanding of the host proteomic changes associated with COVID-19. This will further expand our knowledge about the pathological changes of COVID-19, and provide
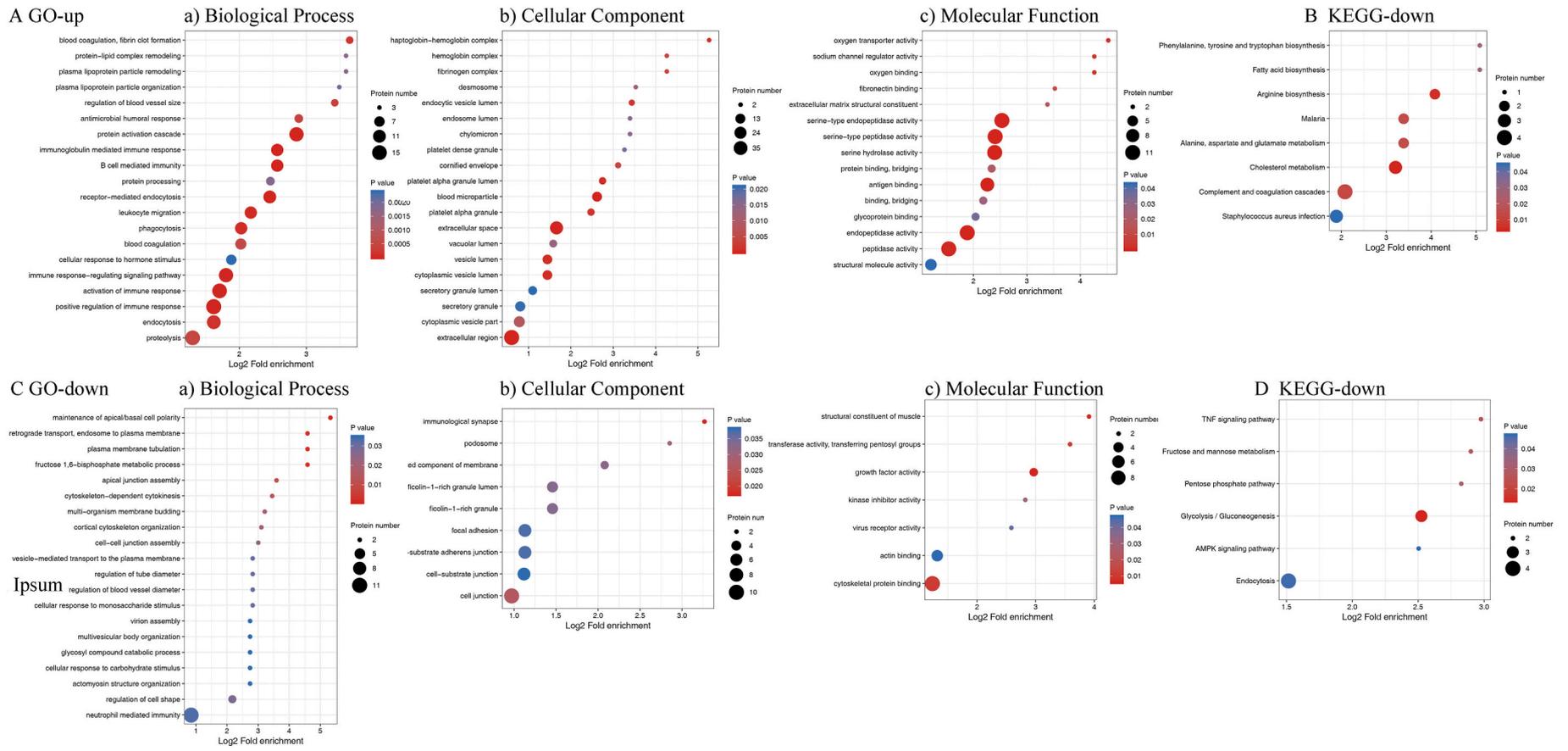
Fig. 6. GO and KEGG enrichment scatter plot of these up- and down-regulated proteins. The y-axis shows significantly enriched GO and pathway terms relative to the network, and the x-axis shows the enrichment scores of these terms. Dot size represents the number of genes, and the colour indicates the p-value. A is the up-regulated proteins and Gene Ontology (GO) annotation for biological process (a), cellular compartment (b), and molecular function (c); B is KEGG pathway analysis for these up-regulated proteins; C is the down-regulated proteins and Gene Ontology (GO) annotation for biological process (a), cellular compartment (b), and molecular function (c); D is KEGG pathway analysis for these down-regulated proteins.

hints of potential therapeutic strategies.

Supplementary data to this article can be found online at https://doi.org/10.1016/j.lfs.2021.119046.

Ethical approval and consent to participate

All the procedures were approved by the Ethics Committee of the First Affiliated Hospital of Guangzhou Medical University (No. 2020-65). Verbal informed consent were obtained from all participants because the family members were in quarantine.

Consent for publication

Not applicable.

Availability of data and materials

The datasets used during the current study are available from the corresponding author on reasonable request.

Funding

CRediT authorship contribution statement

Wenju Lu, Nanshan Zhong, Xiaoqing Liu, Yiming Li and Jincun Zhao conceived and designed the experiments. Fei Liu, Airu Zhu, Yuanyuan Li and Jieping Luo conducted the sample preparation. Zili Zhang, Tao Wang and Guoping Gu conducted the data and bioinformatics analyses. Zili Zhang and Tao Wang wrote the manuscripts. Jieping Luo and Jingyi Xu collected and analyzed the clinical data. Wenju Lu oversaw the completion of this study and edited the manuscript.

Declaration of competing interest

The authors have no conflict of interest to declare.

Acknowledgements

References

[1] Epidemiology Working Group for NCIP Epidemic Response CCfDC and Prevention. [The epidemiological characteristics of an outbreak of 2019 novel coronavirus diseases (COVID-19) in China], Zhonghua Liu Xing Bing Xue Za Zhi 41 (2) (2020) 145–151.

[2] X. Yang, et al., Clinical course and outcomes of critically ill patients with SARS-CoV-2 pneumonia in Wuhan, China: a single-centered, retrospective, observational study, Lancet Respir. Med. 8 (5) (2020) 475–481.

[3] W. Lu, et al., Elevated MUC1 and MUC5AC mucin protein levels in airway mucus of critical ill COVID-19 patients, J. Med. Virol. 93 (2) (2020) 582–584.

[4] F. Wang, et al., Reproducibility of fluid-phase measurements in PBS-treated sputum supernatant of healthy and stable COPD subjects, Int J Chron Obstruct Pulmon Dis 14 (2019) 835–852.

[5] B. Schwanhausser, et al., Global quantification of mammalian gene expression control, Nature 473 (7347) (2011) 337–342.

[6] S.K. Thaker, et al., Viral hijacking of cellular metabolism, BMC Biol. 17 (1) (2019) 59.

[7] M.T. Snaebjornsson, A. Schulze, Non-canonical functions of enzymes facilitate cross-talk between cell metabolic and regulatory pathways, Exp. Mol. Med. 50 (4) (2018), 34.

[8] J. Zhang, Q.M. Chen, Far upstream element binding protein 1: a commander of transcription, translation and beyond, Oncogene 32 (24) (2013) 2907–2916.

[9] R.W. Hunter, et al., Metformin reduces liver glucose production by inhibition of fructose-1-6-bisphosphatase, Nat. Med. 24 (9) (2018) 1395–1406.

[10] Y.C. Chang, et al., Roles of aldolase family genes in human cancers and diseases, Trends Endocrinol. Metab. 29 (8) (2018) 549–559.

[11] C.F. Wang, et al., Differential gene expression of aldolase C (ALDOC) and hypoxic adaptation in chickens, Anim. Genet. 38 (3) (2007) 203–210.

[12] M. Ali, et al., Hereditary fructose intolerance, J. Med. Genet. 35 (5) (1998) 353–365.

[13] J.A. Schatz-Jakobsen, et al., Structural insight into proteolytic activation and regulation of the complement system, Immunol. Rev. 274 (1) (2016) 59–73.

[14] P.H. Pandya, D.S. Wilkes, Complement system in lung disease, Am. J. Respir. Cell Mol. Biol. 51 (4) (2014) 467–473.

[15] V.J. Sarma, et al., Complement in lung disease, Autoimmunity 39 (5) (2006) 387–394.

[16] L.E. Gralinski, et al., Complement activation contributes to severe acute respiratory syndrome coronavirus pathogenesis, mBio 9 (5) (2018).

[17] M. Kuang, et al., FGB and FGG derived from plasma exosomes as potential biomarkers to distinguish benign from malignant pulmonary nodules, Clin. Exp. Med. 19 (4) (2019) 557–564.

[18] X. Li, et al., Risk factors for severity and mortality in adult COVID-19 inpatients in Wuhan, J. Allergy Clin. Immunol. 146 (1) (2020) 110–118.

[19] M. Drent, et al., Usefulness of lactate dehydrogenase and its isoenzymes as indicators of lung damage or inflammation, Eur. Respir. J. 9 (8) (1996) 1736–1742.

[20] E. Lopez-Collazo, et al., Immune response and COVID-19: a mirror image of sepsis, Int. J. Biol. Sci. 16 (14) (2020) 2479–2489.

[21] B.M. Henry, et al., Lactate dehydrogenase levels predict coronavirus disease 2019 (COVID-19) severity and mortality: a pooled analysis, Am. J. Emerg. Med. 38 (9) (2020) 1722–1726.

[22] E.J. Favaloro, J. Thachil, Reporting of D-dimer data in COVID-19: some confusion and potential for misinformation, Clin. Chem. Lab. Med. 58 (8) (2020) 1191–1199.

[23] B.M. Henry, et al., Hematologic, biochemical and immune biomarker abnormalities associated with severe illness and mortality in coronavirus disease 2019 (COVID-19): a meta-analysis, Clin. Chem. Lab. Med. 58 (7) (2020) 1021–1028.

[24] D. McGonagle, et al., The role of cytokines including interleukin-6 in COVID-19 induced pneumonia and macrophage activation syndrome-like disease, Autoimmun. Rev. 19 (6) (2020), 102537.